Heliyon 10 (2024) e37002

Contents lists available at ScienceDirect

Heliyon

journal homepage: www.cell.com/heliyon

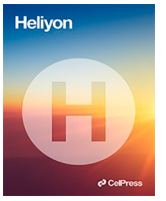

Research article

Human umbilical cord mesenchymal stem cell-derived exosomes mitigate diabetic nephropathy via enhancing M2 macrophages polarization

Xueting Li [a], Mingkai Chen [b], Jinghe Cao [c], Xinke Chen [b], Hui Song [b], Shuo Shi [b], Baoyu He [b], Bin Zhang [b,**], Ziteng Zhang [d,e,*]

[a] *Department of Nephrology, Affiliated Hospital of Jining Medical University, Jining, Shandong, PR China*
[b] *Department of Laboratory Medicine, Affiliated Hospital of Jining Medical University, Jining Medical University, Jining, Shandong, PR China*
[c] *Department of Reproductive Center, Affiliated Hospital of Jining Medical University, Jining Medical University, Jining, Shandong, PR China*
[d] *Departments of Thoracic Surgery, Affiliated Hospital of Jining Medical University, Jining, Shandong, 272000, PR China*
[e] *Departments of Thoracic Surgery, Qinghai Red Cross Hospital, Xining, Qinghai, 81000, PR China*

ARTICLE INFO

Keywords:
Human umbilical cord mesenchymal stem cells
Exosomes
Diabetic kidney disease
Single-cell transcriptome sequencing
M2 macrophages polarization

ABSTRACT

Background and objectives: Exosomes, which are small nanoscale vesicles capable of secretion, have garnered significant attention in recent years because of their therapeutic potential, particularly in the context of kidney diseases. Notably, human umbilical cord mesenchymal stem cell-derived exosomes (hucMSC-Exos) are emerging as promising targeted therapies for renal conditions. The aim of this study was to investigate the therapeutic effects of hucMSC-Exos on diabetic kidney disease (DKD) both in vivo and in vitro. Additionally, this study seeks to elucidate cellular and molecular differentials, as well as the expression of relevant signaling pathways, through single-cell RNA sequencing. This endeavor was designed to enhance our understanding of the connection between hucMSC-Exos and the pathogenesis of DKD.

Methods and results: The study commenced with the extraction and characterization of hucMSC-Exos, including the determination of their concentrations. Animal experiments were conducted to evaluate the therapeutic potential of hucMSC-Exos in a DKD mouse model. Subsequently, single-cell sequencing was employed to investigate the molecular mechanisms underlying the efficacy of extracellular vesicles in ameliorating DKD. These findings were further substantiated by cell-based experiments. Importantly, the results indicate that hucMSC-Exos can impede the progression of DKD in mice, with macrophage activation playing a pivotal role in this process.

Conclusions: The in vivo experiments conclusively established hucMSC-Exos as a pivotal component in preserving renal function and retarding the progression of DKD. Our utilization of single-cell sequencing technology, in conjunction with in vivo and in vitro experiments, provides compelling evidence that M2 macrophages are instrumental in enhancing the amelioration of diabetic nephropathy.

* Corresponding author. Departments of Thoracic Surgery, Affiliated Hospital of Jining Medical University, Jining, Shandong 272000, PR China.
** Corresponding author.
E-mail addresses: zhangbin@mail.jnmc.edu.cn (B. Zhang), zitengzhang1353@163.com (Z. Zhang).

https://doi.org/10.1016/j.heliyon.2024.e37002
Received 27 February 2024; Received in revised form 21 August 2024; Accepted 26 August 2024
Available online 28 August 2024

1. Introduction

Diabetic kidney disease (DKD) is the most prevalent complication in the spectrum of diabetes-related microvascular disorders and has emerged in recent decades as a primary contributor to the onset of end-stage renal disease [1]. The pathogenesis of DKD is rooted in the damage inflicted upon renal microvessels in a hyperglycemic environment, resulting in increased pressure in renal blood vessels, glomerulosclerosis, and a decline in the glomerular filtration rate [2]. Currently, no specific pharmacological intervention has been identified for DKD, underscoring the imperative need to explore novel and effective therapeutic strategies to mitigate its progression.

Human umbilical cord mesenchymal stem cells (hucMSCs) have emerged as promising candidates because of their noninvasive isolation, low immunogenicity, rapid self-renewal capacity, and efficient proliferative potential. These attributes have led to their widespread adoption in the medical domain [3]. Within this context, exosomes have emerged as noteworthy constituents, representing a category of small, single-membraned, nanoscale vesicles with complex structural and compositional diversity, encompassing DNA fragments, circular RNAs (cirRNAs), messenger RNAs (mRNA), lipids, and proteins [4]. Exosomes are primarily secreted through the fusion of endosomal vesicles with the plasma membrane, releasing their internal vesicles into the extracellular environment [5]. They function predominantly via receptor binding to target cells, facilitating the transfer of cargo and enabling comprehensive cellular

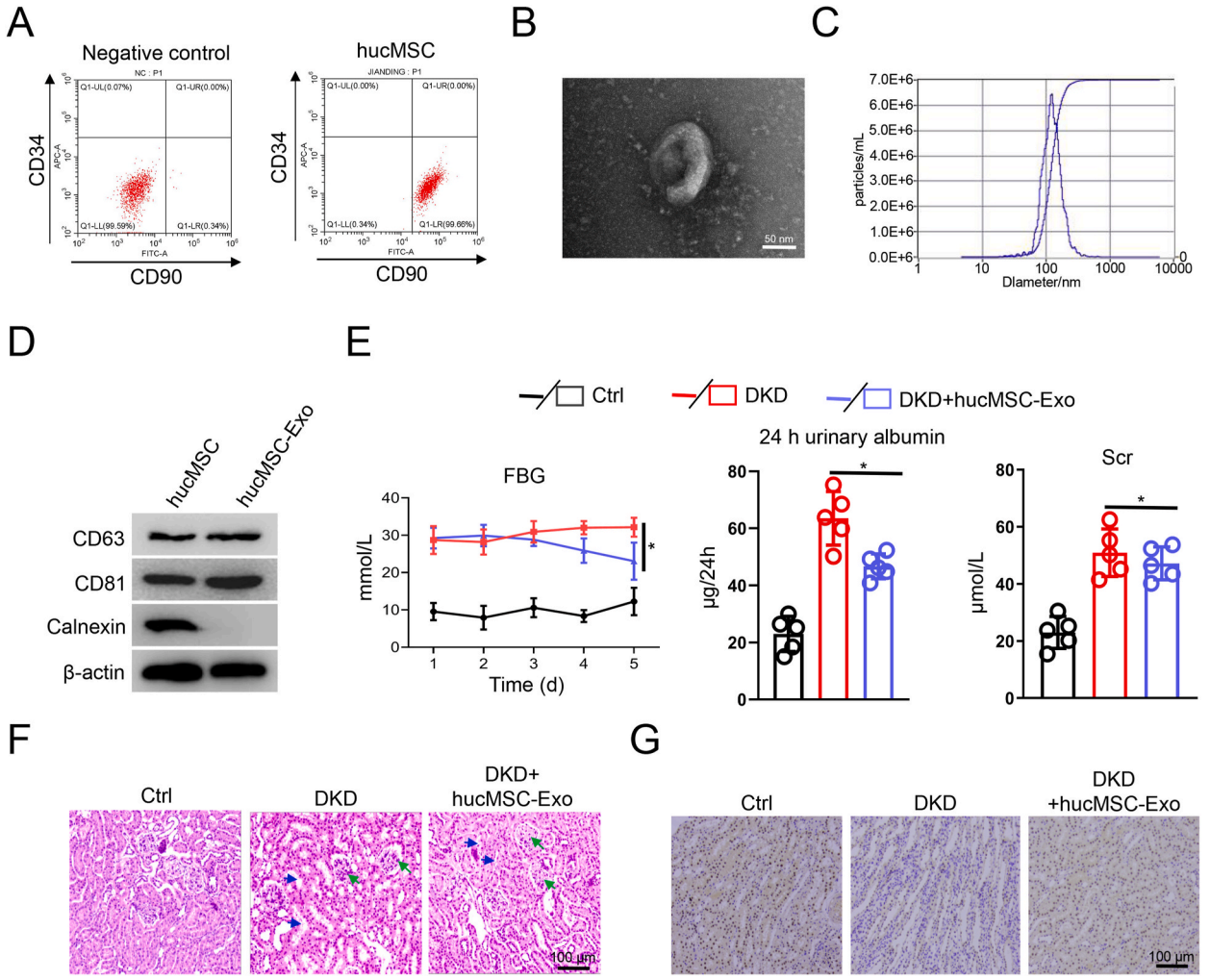

Fig. 1. Effects of HucMSC-Exo on renal indicators in the control, DKD, and DKD + hucMSC-Exo mice.
(A) characterization of hucMSCs using flow analysis with positive marker CD90 and native marker CD34. (B) Electron micrograph showing the morphology of hucMSC-Exo. (C) Particle size distribution of hucMSC-Exo. (D) Western blot analysis demonstrating the expression of two transmembrane proteins (CD63 and CD81), a negative control (Calnexin). β-actin serves as cell internal reference in hucMSC-Cell and hucMSC-Exo. (E) Changes in FBG, 24-h urinary albumin excretion rate, and Scr in the Control group, DKD group, and DKD + hucMSC-Exo group. (F) H&E staining of kidney tissues in the NC group, DKD group, and DKD + hucMSC-Exo group. (G) Immunohistochemical analysis of Ki67 expression in kidney tissues of mice from each group.
Note: NC, control group; DKD, diabetic nephropathy group; DKD + hucMSC-Exo group, diabetic nephropathy group treated with hucMSC-Exo. *p < 0.05, **p < 0.01, ***p < 0.001.

communication and information exchange [6]. Recent studies have highlighted the therapeutic potential of extracellular vesicles originating from human umbilical cord mesenchymal stem cells as a targeted treatment strategy for kidney-related maladies [7].

Macrophages, ubiquitous immune cells in the human body, can be categorized into two main phenotypes: M1 (classically activated macrophages) and M2 (alternatively activated macrophages [8]. Among these, M2 macrophages play a pivotal role in dampening inflammatory processes, promoting tissue repair, remodeling, angiogenesis in damaged tissues, and maintaining internal homeostasis [9]. Notably, a substantial number of macrophages are involved in DKD pathogenesis. However, it remains an unresolved query whether human umbilical cord mesenchymal stem cell-derived exosomes (hucMSC-Exo) can ameliorate the inflammatory response associated with DKD by modulating macrophage activity, necessitating experimental validation [10].

In recent decades, the application of advanced tools such as bioinformatics to investigate gene expression profiles at the population level has gained widespread acceptance. The advent of single-cell RNA sequencing (scRNA-seq) has ushered in an era in which we can scrutinize gene expression profiles at the granularity of individual cells [11]. Currently, scRNA-seq has become an effective biological tool for the comprehensive investigation of thousands of genes at the single-cell level and is utilized for diverse applications, including cell type identification, quantification of global gene expression heterogeneity across cells, and evaluation of cellular responses [12]. Furthermore, this technology has been instrumental in elucidating matters related to gene expression regulation and intracellular signal transduction pathways in individual cells [13]. The present study leverages scRNA-seq to probe the potential of hucMSC-Exos in ameliorating DKD through the modulation of macrophage activity. Our objective was to delineate the molecular mechanism of DKD and elucidate novel and effective therapeutic modalities with a focus on this pathogenic condition.

2. Results

2.1. Impacts of hucMSC-Exo on the disease process in DKD mice

First, we characterized the hucMSCs using flow cytometry with the positive marker CD90 and native marker CD34 (Fig. 1A). Next, we isolated and characterized hucMSC-Exos by microscopy and immunoblotting. Transmission electron microscopy revealed hucMSC-Exos as disc-shaped vesicles (Fig. 1B). The particle size of hucMSC-Exos was analyzed using Nanoparticle Tracking Analysis (NTA) technology (Fig. 1C), revealing that the majority of hucMSC-Exo particles had a size of 100–200 nm. Western blotting results demonstrated the positive expression of two transmembrane proteins, CD81 and CD63, and the negative expression of the endoplasmic reticulum marker calnexin in hucMSC-Exo (Fig. 1D).

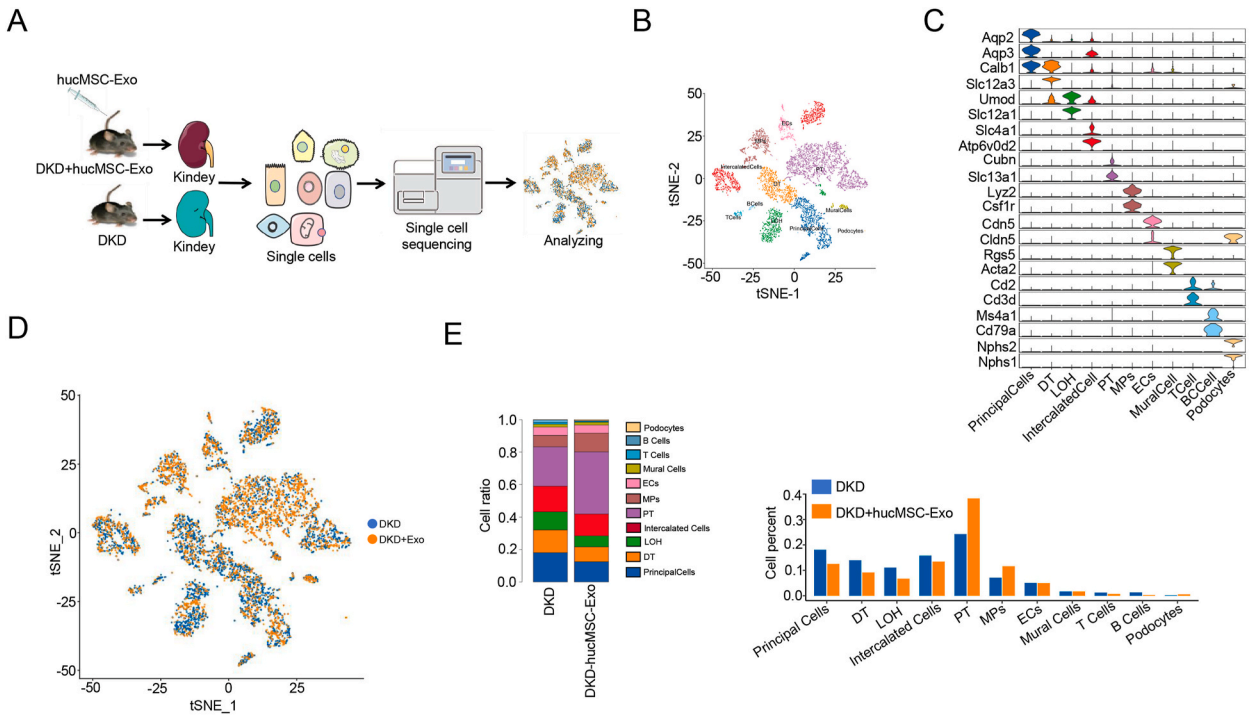

Fig. 2. Overview of kidney cell isolates from DKD mice and DKD + hucMSC-Exo mice.
(A) Schematic representation of the single-cell sequencing process. (B) TSNE maps of all cells in the DKD group and DKD + hucMSC-Exo group. (C) Violin plots illustrating gene expression in the DKD group and DKD + hucMSC-Exo group. (D) t-SNE plots depicting cell proportions in the DKD group and DKD + hucMSC-Exo group. (E) Bar chart displaying cell proportions in the DKD group and DKD + hucMSC-Exo group.
Note: NC, control group; DKD, diabetic nephropathy group; DKD + hucMSC-Exo group, diabetic nephropathy group after hucMSC-Exo treatment.

Nest, we established the DKD model. As shown in Fig. 1E, a conspicuous increase in FBG, BW, and 24-h urinary albumin excretion rates were observed in the DKD group compared with the NC group ($p < 0.001$). After 8 weeks of treatment, the DKD + hucMSC-Exo group exhibited a reduction in FBG ($p < 0.05$) and a decrease in the 24-h urinary albumin excretion rate ($p < 0.05$). HE staining (Fig. 1F) revealed notable vacuolar degeneration in the renal tubules of the DKD group, along with thickening of the glomerular matrix, reduced glomerular volume, improved mesangial area dilation, and diminished tubular vacuolar degeneration in the DKD +

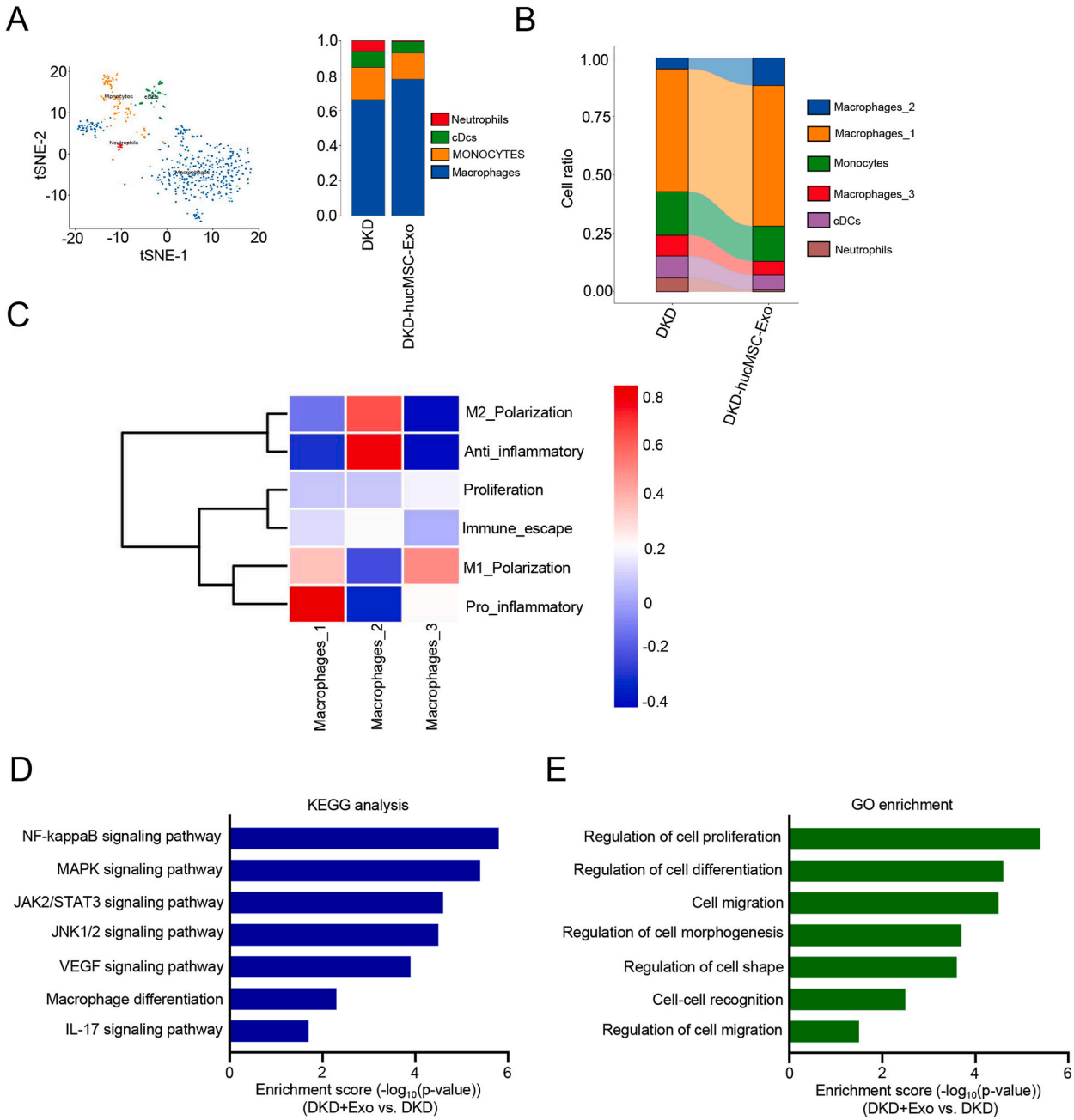

Fig. 3. Single cell sequencing analysis of changes in myeloid immune cells following hucMSC-Exo treatment.
(A) t-SNE maps of all immune cells in the DKD group and DKD + hucMSC-Exo group. (B) Proportion diagram illustrating macrophage distribution in the DKD group and DKD + hucMSC-Exo group. (C) GSVA plots of M2 and non-M2 macrophages. (D and E) KEGG analysis (D) and GO enrichment analysis (E) using differentially expressed genes in macrophages from single-cell sequencing data of kidney tissues in DKD and hucMSC Exo + DKD mice. p-values <0.05 were defined as statistically significant. The vertical axis represents the pathway category or biological procession category, and the horizontal axis represents the-$\log_{10}$(p-value) of these significant pathways or biological processes.
Note: DKD, diabetic nephropathy group; DKD + hucMSC-Exo group, diabetic nephropathy group after hucMSC-Exo treatment; M2 cells, type II macrophages.

hucMSC-Exo group compared to the DKD group. Immunohistochemical results (Fig. 1G) demonstrated a significantly diminished positive rate of Ki67 in the DKD group compared with the NC group, indicative of reduced renal cell proliferation activity. In contrast, the DKD + hucMSC-Exo group exhibited a significantly increased positive rate of Ki67 compared to the DKD group.

2.2. *Single-cell RNA sequencing data reveal the differential cell subpopulation in kidney tissues from mice treated with hucMSC-Exo*

As shown in Fig. 2A, kidney cells were dissociated from both the DKD and DKD + hucMSC-Exo groups, resulting in 6989 single cells. The genetic material in these cells was reverse transcribed into cDNA, followed by PCR amplification, high-throughput sequencing, and associated data analysis. Subsequently, we employed for dimensionality reduction analysis, as illustrated in Fig. 2B, to assess the comprehensive classification and distribution of cells in each group. To provide further insights, we used violin plots to visualize gene expression across all cells in various clusters (Fig. 2C). Dimensionality reduction fluoroscopy was once again applied to analyze the cell composition of the DKD and DKD + hucMSC-Exo groups using tSNE annotation cluster images, as shown in Fig. 2D. To offer a more intuitive representation, a bar chart was used to illustrate the proportion of each cell cluster in both the DKD and DKD + hucMSC-Exo groups (Fig. 2E).

2.3. *M2 macrophages polarization is involved in hucMSC-Exo-mediated DKD alleviation*

To investigate immune cell alterations in the DKD and DKD + hucMSC-Exo groups, we employed single-cell RNA sequencing (scRNA-seq) to create tSNE dimensionality reduction maps encompassing all immune cells in both groups, as illustrated in Fig. 3A. To identify the specific immune cell population that exhibited the most significant changes following hucMSC-Exo treatment, we constructed a histogram illustrating the proportions of various cell types in both the DKD and DKD + hucMSC-Exo groups (Fig. 3B). This graphical representation reveals an increase in the proportion of Macrophage-2 cells upon hucMSC-Exo administration. To gain deeper insights into the functional characteristics of Macrophage-2 cells and their relationship with macrophages, we conducted GSVA enrichment analysis. In this analysis, the y-axis represents pathways and the x-axis represents cell types, with red indicating high pathway activity and blue indicating low pathway activity. The results of this analysis demonstrated a notable overlap between Macrophage-2 cells and M2 cells (Fig. 3C), providing strong evidence that Macrophage-2 cells are indeed a subset of M2 cells. Next, Kyoto Encyclopedia of Genes and Genomes (KEGG) pathway analysis and gene ontology term enrichment (GO) were performed for the

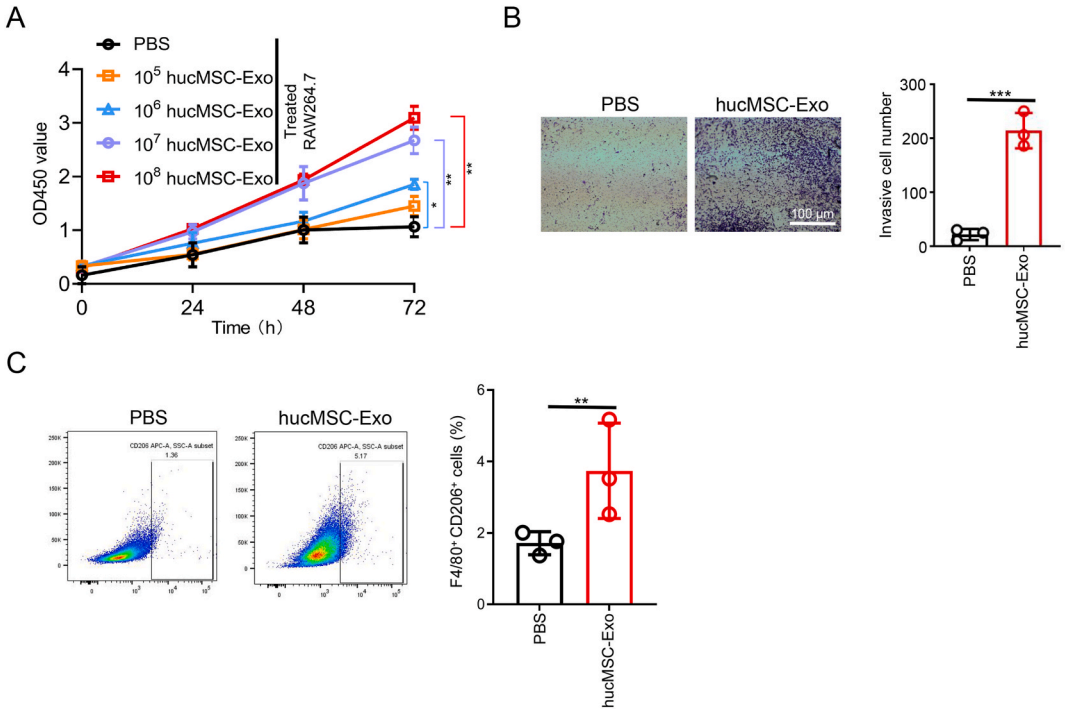

Fig. 4. *In-vitro* and *in-vivo* experiments confirm the role of hucMSC-Exo in M2 activation.
(A) CCK-8 assay showing the effect of different concentrations of hucMSC-Exo on RAW264.7 cells. (B) Transwell experiment demonstrating the impact of hucMSC-Exo on RAW264.7 cells. (C) Flow cytometry analysis of M2 cell surface markers (F4/80 + CD206+) in RAW and RAW + hucMSC-Exo groups.
Note: NC, control group; DKD, diabetic nephropathy group; DKD + hucMSC-Exo group, diabetic nephropathy group after hucMSC-Exo treatment; RAW group, macrophage group; RAW + hucMSC-Exo group, macrophage group after hucMSC-Exo treatment; M2 cells, type II macrophages. *$p < 0.05$, **$p < 0.01$, ***$p < 0.001$.

potential mechanism and pathways that hucMSC-Exo may involved in macrophage using differential genes. The KEGG enrichment analysis revealed that the differentially expressed genes in macrophage from hucMSC-Exo + DKD kidney were primarily associated with 'NF-kappaB signaling pathway', 'MAPK signaling pathway', 'JAK2/STAT3 signaling pathway', and 'JNK1/2 signaling pathway' (Fig. 3D). The GO analysis displayed that 'Regulation of cell proliferation', 'Regulation of cell differentiation', 'Regulation of cell morphogenesis', 'Cell-cell recognition', and 'Regulation of cell migration' were potentiated in macrophage from hucMSC-Exo + DKD kidney (Fig. 3E). Collectively, this data substantially support the involvement of M2 macrophages in the process by which hucMSC-Exos alleviate the progression of DKD.

2.4. Validation of hucMSC-Exo as a key mediator of macrophage activation through both in-vitro and in-vivo experiments

The findings derived from the single-cell sequencing analysis suggest the involvement of macrophage activation in impeding the progression of DKD. To ascertain whether hucMSC-Exos can induce macrophage polarization towards the M2 phenotype and contribute to the mitigation of DKD progression, a series of experiments were conducted. In the in vitro experiments, RAW264.7 cells were cultured and exposed to varying concentrations, specifically 10^5/ml, 10^6/ml, 10^7/ml, and 10^8/ml. Cellular proliferation was assessed using a CCK8 assay (Fig. 4A), which revealed a significant increase in RAW264.7 the proliferation of hucMSC-Exo administration. Notably, the most effective concentration for hucMSC-Exo–induced proliferation was determined to be 10^8/ml. Subsequently, a Transwell migration assay (Fig. 4B) demonstrated a substantial increase in the number of macrophages traversing the basement membrane in response to hucMSC-Exo stimulation at a concentration of 10^8/ml, demonstrating a statistically significant difference ($p < 0.001$). Furthermore, flow cytometry analysis (Fig. 4C) revealed a noteworthy increase in the surface markers (F4/80 + CD206+) of M2 macrophages in the hucMSC-Exo-treated RAW264.7 cells compared to PBS-treated RAW264.7 cells. These results collectively validate the capacity of hucMSC-Exos to induce the polarization of macrophages towards the M2 phenotype, thereby underscoring their pivotal role in alleviating the progression of DKD.

3. Discussion

DKD is a prevalent chronic condition, and a comprehensive understanding of its etiology remains elusive. Prior research indicates a plausible association between DKD pathogenesis and factors such as advanced glycation end-product formation, the release of related inflammatory mediators, immune system dysregulation, and oxidative stress [14]. Extracellular vesicles, known as hucMSC-Exos, encapsulated by lipid bilayer membranes, play a pivotal role in intercellular communication [15]. Currently, hucMSC-Exos have demonstrated significance across various aspects, including tumor diagnostics, migration and proliferation, tissue damage repair, immune antigen presentation, and neurodegenerative research [16]. Recently, MSC-derived exosomes have attracted much attention for their ability to facilitate renal repair and potential for DKD therapy [17,18]. Studies underscore the involvement of hucMSC-Exos, which carry miRNAs and long non-coding RNAs, in diabetes progression, positioning them not only as potential early diagnostic markers for DKD but also as contributors to its pathogenesis [19]. As a key secretory product of MSCs, exosomes shuttle various proteins, messenger RNAs (mRNAs), and microRNAs (miRNAs) to modulate the activity of recipient cells, thereby playing important roles in kidney diseases such as DKD and acute kidney injury (AKI) [20,21]. The emerging technology of single-cell sequencing, a valuable tool for investigating intercellular signaling in various diseases including cancer [22], was employed in this study to investigate the molecular and cellular effects and mechanisms of hucMSC-Exo on DKD.

Our experimental model employed db/db mice as the DKD model, and db/m mice as the control group. Following a 10-week regimen of high-fat and high-sugar diet, continuous monitoring of body weight, blood glucose levels, and urinary microalbumin excretion was conducted. Upon successful establishment of the DKD model, mice were divided into two groups: one receiving hucMSC-Exo via tail vein injection and the other receiving an equivalent volume of PBS. After 8 weeks, the mice were euthanized, and FBG, Scr, 24-h urinary albumin excretion rate, BW, BUN, and other indicators were assessed. Notably, FBG, Scr, and 24-h urinary albumin excretion rates were significantly reduced compared to those in the DKD group. Histological examinations, including HE staining and Ki67 immunohistochemistry, further demonstrated marked improvement in renal tissue with hucMSC-Exo administration compared to the DKD group. Collectively, these findings provide compelling evidence supporting the ability of hucMSC-Exos to ameliorate DKD.

The mechanisms through which MSC-derived exosomes exert their therapeutic effects are multifaceted. DKD is an inflammatory disease, and the activation and infiltration of macrophages play important roles in its occurrence and development [23,24]. Several studies have shown that polarization of M1/M2 macrophages is closely related to the occurrence and progression of DKD [25–27]. Elevated glucose levels not only impact renal tissue but also significantly alter the cellular composition of the kidney. Under hyperglycemic conditions, the immune system is predisposed to dysfunction, contributing to insulin resistance, triggering oxidative stress, and facilitating the release of inflammatory factors [28]. As crucial regulators of the immune system, macrophages can activate vascular endothelial cells in high-glucose environments, inducing upregulation of cell adhesion molecules and chemokines. This leads to enhanced secretion of diverse inflammatory factors by macrophages, culminating in kidney tissue damage [29]. Our investigation, utilizing single-cell sequencing alongside in vitro and in vivo experiments, validates that hucMSC-Exos can induce macrophage activation into the M2 phenotype, thereby impeding the progression of DKD.

In conclusion, our study provides the compelling evidence regarding the efficacy of hucMSC-Exos in ameliorating DKD in vivo and introduces a novel approach to DKD clinical treatment. Moreover, the therapeutic effect was mediated by the activation of macrophages by hucMSC-Exos. However, several limitations of this study merit consideration: (1) Lack of Organ Targeting: One limitation pertains to the absence of explicit organ targeting by the extracellular vesicles. Injected extracellular vesicles do not exhibit direct kidney-specific homing following systemic circulation, thereby raising questions regarding the extent to which hucMSC-Exos exert

their functions in renal tissue. To address this, future investigations may utilize in vivo fluorescence detection technology to elucidate the precise distribution of hucMSC-Exos in the kidneys of mice receiving hucMSC-Exo injections. (2) Limited Comparative Analysis: In study, our analysis was restricted to the differences observed in single-cell sequencing between the DKD and DKD + hucMSC-Exo groups. To enhance the comprehensiveness of our findings, incorporating single-cell sequencing data from the NC group for comparative analysis would be beneficial. This expanded dataset could offer a more comprehensive understanding of alterations in cellular molecular expression induced by hucMSC-Exo treatment, thereby elucidating the underlying mechanisms of signal transduction. (3) Superficial Examination of Signal Transduction Pathways: Another limitation pertains to the lack of in-depth exploration of the signal transduction pathways involved in the processes described above. To overcome this limitation, future research efforts will delve into the intricate molecular mechanisms by which macrophages influence hucMSC-Exos, ultimately enhancing our understanding of how these interactions facilitate the amelioration of Diabetic Nephropathy. In future studies, we aim to conduct a more thorough investigation into the molecular mechanisms underlying the interaction between macrophages and hucMSC-Exos, ultimately elucidating the intricate signaling pathways that drive the therapeutic effects on DKD.

4. Materials and methods

4.1. Animals

In this study, the DKD model was established using spontaneous diabetic mice (db/db mice), with db/m mice as controls. Ten male db/db mice and five male db/m mice, approximately six weeks old and weighing approximately 50 ± 10 g, were procured from Jiangsu Jicui Yaokang Biotechnology Co., Ltd. These mice were a 7-day acclimation period and housed at the SPF level in the Animal Center of Jining Medical College (approval no. 2020C023). All animal experiments complied with the ARRIVE guidelines and were carried out in accordance with the U.K. Animals (Scientific Procedures) Act, 1986 and associated guidelines. The model group was fed a high-sugar and high-fat diet, whereas the control group was fed a standard diet. The bedding was replaced daily, water was regularly refreshed, and feed was replenished as needed. Over the course of 10 weeks, blood glucose levels were monitored weekly and urine was collected at regular intervals using a mouse metabolic cage to assess microalbumin levels. The DKD mouse model was validated when the model group exhibited characteristics such as a weakened mental state, sparse and coarse fur, a significant increase in food and water consumption, sustained fasting blood glucose levels of $\geq$16.7 mmol/L, and a notably higher 24-h urinary albumin excretion rate than the NC group [30]. Subsequently, the successfully modeled DKD mice were randomly divided into two groups, the DKD group and the DKD + hucMSC-Exo group, each consisting of five mice. An equal number of db/m mice were used as controls. The DKD + hucMSC-Exo group received 10 mg/kg of hucMSC-Exo three times a week for 8 weeks, whereas the DKD and control groups were administered an equivalent volume of PBS via tail vein injections. The injection procedure involved immersing the mouse tail in warm water to dilate the tail vein, securing the tail in a specialized instrument for tail vein injections, and immobilizing the tail vein using a pulse clamp under yellow light after locating the clear tail vein. The tail vein was disinfected with an alcohol swab, and once blood return from the needle tip was observed, signifying successful entry into the tail vein, the pulse clamp was released [31]. Throughout the injection period, body weight (BW) and fasting blood glucose (FBG) levels were assessed every two weeks. All mice were euthanized and sample testing was conducted at 18 weeks.

4.2. Cell culture and treatment

Mouse macrophage cells **(**RAW264.7) (BK-X63399, Biotech Supply, Shanghai, China) were utilized for in vitro experimental validation. Dulbecco's modified Eagle's medium (DMEM) with low glucose (5.6 mmol/L) was used for cell culture.

4.3. Isolation and characterization of hucMSC-Exo

All participants provided informed consent for the use of umbilical cords, and the study received ethical approval from the Affiliated Hospital of Jining Medical College (approval no. 2020C023). DMEM was used for cultivation of human umbilical cord stem cells [31,32]. HucMSCs were cultured until the third generation. When the P3 generation cells reached 80 %–90 %, 20 mL serum-free medium was added, and the cells were cultured for 48 h. The cell supernatant was collected for extraction of extracellular vesicles. Using high-speed centrifugation, the extraction of hucMSC-Exos from conditioned MSC cultures adhered to the protocol outlined by Zhang Y et al. [33]. In brief, following a 5-min centrifugation at 1500×*g* to eliminate cell debris, the supernatant underwent for another 1-h centrifugation at 100,000×*g* at 4 °C to isolate the ultimate exosome fraction. The protein content was determined using the BCA Protein Assay Kit (Shanghai, China) [34]. Transmission electron microscopy was used to inspect the morphology of the isolated exosomes. The presence of CD81 and CD63 on the exosome surface was assessed using immunoblotting.

4.4. Histological staining

After an 8-week treatment period that included both administration of normal saline and the designated treatment, the rats were euthanized. The kidneys of each mouse were extracted and the kidney tissue was thoroughly cleaned using phosphate-buffered saline (PBS). Kidney tissue was underwent for 48-h fixation period in 4 % paraformaldehyde, followed by embedding in paraffin. Sections (5 μm each) were prepared and subjected to hematoxylin and eosin (HE) staining (G1003, Servicebio). Image analysis, facilitated by ImageJ software (National Institutes of Health, Maryland, USA), was employed to evaluate structural alterations in both glomeruli and

renal tubules.

4.5. Immunohistochemical staining

To assess the expression of Ki67 in the kidney tissue, immunohistochemical analysis was conducted using anti-Ki67 antibodies (ab279653, Servicebio, Wuhan, China) and secondary antibodies (GB12008, Servicebio, Wuhan, China). Briefly, following the dewaxing and antigen retrieval steps, the paraffin-embedded sections were immersed in 3 % hydrogen peroxide for 25 min at room temperature. Subsequent steps comprised overnight incubation (16–18 h) at 4 °C with primary antibodies and incubation at room temperature for 50-min incubation with secondary antibodies. Sequential staining was performed using diaminobenzidine and hematoxylin (Servicebio, Wuhan, China). Following adequate drying, the slides were captured and analyzed using ImageJ software.

4.6. Western blot

Western blot analysis was performed using standard techniques. Anti-β-actin antibody (Cell Signaling Technology, #4967) was used as a control. Primary antibodies against CD63 (Abcam, #ab134045), CD81 (Cell Signaling Technology, #56039), and calnexin (Cell Signaling Technology, #2433) were used. The signal was visualized using an ECL detection reagent and quantified by densitometry using the ImageJ software (http://rsb.info.nih.gov/ij).

4.7. Cell viability assay

After seeding RAW264.7 cells (1×10^4 cells/well/100 μl) into a 96-well plate and culturing overnight, CCK8 (10 μl) was applied to each well, followed by measurement of absorbance at 450 nm using a spectrophotometer (Quant spectrophotometer, Bio-Tek Instruments, Winooski, VT) at specified time intervals of 0 h, 24 h, and 36 h.

4.8. Transwell migration assay

Utilizing 24-well plates with various compositions of 5 % FBS, RAW264.7 cells were accommodated on Transwell inserts (1×10^5 cells/well/100 μl, pore size of 8 μm, Thermo Fisher Scientific). After 24-h of treatment, the cells were fixed using 2 % paraformaldehyde, permeabilized using 0.01 % Triton X-100 (Sigma-Aldrich), and stained with crystal violet (Sigma-Aldrich). Delicate removal of non-migrated cells from the transwell membrane was conducted using cotton swabs [35]. Visualization of migrated cells was carried out using a phase-contrast microscope (Olympus BX51-FL-CCD), and capture was facilitated by an Olympus XC50 camera in conjunction with anaLYSIS software. Analysis of the results was conducted using ImageJ software.

4.9. Flow cytometry analysis

In a 24-well plate, RAW264.7 cells were seeded and cultured overnight. The cells were then incubated with LPS (Beyotime, Shanghai, China) and various concentrations of AA for 24 h, harvested, and incubated with F4/80 and CD206 antibodies (Elabscience) for 30 min at 4 °C. After three washes with PBS, cells were resuspended for flow cytometry analysis.

4.10. Single-cell RNA sequencing

Utilizing CeleScope v1.5.2 (Singleron Biotechnologies) with default parameters, gene expression profiles were generated through the processing of raw reads. Extraction and correction of barcodes and unique molecular identifiers (UMIs) were conducted on R1 reads. Subsequently, R2 reads, with adapter sequences and poly A tails removed, were aligned against the GRCh38 (hg38) (GRCm38 (mm10)) transcriptome employing STAR (v2.6.1b). FeatureCounts(v2.0.1) were then applied to assign uniquely mapped reads to the exons. The gene expression matrix for subsequent analyses was created by merging reads that were successfully assigned and shared the same cell barcode, UMI, and gene. Single-cell RNA sequencing data have been deposited in the Genome Sequence Archive (https://ngdc.cncb.ac.cn/gsa/) and can be accessed via the GSA Series accession number CRA013587.

4.10.1. Differentially expressed genes (DEGs) analysis (using seurat)

DEGs were identified using the Seurat FindMarkers function by employing the Wilcoxon rank-sum test with default parameters [36]. Genes meeting the criteria for DEGs were those expressed in more than 10 % of cells in both groups, exhibiting an average log (Fold Change) value of 0.25. The adjusted p-values were calculated using the Bonferroni Correction, with a significance threshold set at 0.05, to assess statistical significance.

4.10.2. Pathway enrichment analysis

The exploration of potential DEG functions was performed using Kyoto Encyclopedia of Genes and Genomes (KEGG) and Gene Ontology (GO) analyses utilizing version 3.16.1 of the "clusterProfiler" R package [37]. Pathways characterized by a p_adj value falling below 0.05 were deemed as having significant enrichment. Graphical representation through bar plots visually conveys the identified pathways of significance. Within the context of GO, reference gene sets encompassed categories delineated as cellular components (CC), biological processes (BP), and molecular functions (MF).

4.11. Statistical analysis

Data are expressed as mean ± standard error of the mean (SEM). GraphPad Prism version 8.2.1 (GraphPad Software LLC, San Diego, CA, USA) and SPSS 26 (SPSS Inc., Chicago, IL, USA), one-way analysis of variance was performed, accompanied by either the Dunnett T3 post-hoc test in cases of unequal variances or the Tukey post-hoc test for cases characterized by homogeneous variance. The significance threshold was set at $p < 0.05$.

Ethics approval and consent to participate

This study was approved by the ethical approval from the Affiliated Hospital of Jining Medical College (approval no. 2020C023), as well as the informed consent was obtained from all the participants in accordance with the national legislation and the Declaration of Helsinki.

Funding

This study was supported by grants from the National Natural Science Foundation of China, China (No. 82173371, 82273447, 82273069), Project funded by the China Postdoctoral Science Foundation, China (No. 2022M711322), Tai Shan Young Scholar Foundation of Shandong Province (No. tsqn201909192), Shandong Postdoctoral Innovation Project, China (No. SDCX-ZG-202201002). Qinghai Province Central Guiding Local Science and Technology Development Fund Project, China (No. 2023ZY002).

Data availability statement

Original/source data of the scRNA-sequencing were deposited in the Genome Sequence Archive (GSA, https://ngdc.cncb.ac.cn/gsa/) and can be accessed via the GSA Series accession number CRA013587. Any additional information required to re-analyze the data reported in this paper is available from the corresponding authors upon reasonable request.

CRediT authorship contribution statement

Xueting Li: Software, Resources, Methodology, Investigation. **Mingkai Chen:** Project administration, Methodology, Investigation, Funding acquisition. **Jinghe Cao:** Visualization, Validation, Supervision, Investigation, Conceptualization. **Xinke Chen:** Visualization, Validation, Supervision. **Hui Song:** Writing – original draft, Software, Methodology, Investigation. **Shuo Shi:** Visualization, Validation, Investigation, Data curation. **Baoyu He:** Writing – original draft, Validation, Supervision, Funding acquisition. **Bin Zhang:** Writing – original draft, Visualization, Project administration, Funding acquisition. **Ziteng Zhang:** Writing – review & editing, Writing – original draft, Funding acquisition, Conceptualization.

Declaration of competing interest

The authors declare that they have no known competing financial interests or personal relationships that could have appeared to influence the work reported in this paper.

Appendix A. Supplementary data

Supplementary data to this article can be found online at https://doi.org/10.1016/j.heliyon.2024.e37002.

References

[1] J. Barrera-Chimal, F. Jaisser, H.J. Anders, The mineralocorticoid receptor in chronic kidney disease, Br. J. Pharmacol. 179 (13) (2022) 3152–3164.
[2] C. Schiborn, M.B. Schulze, Precision prognostics for the development of complications in diabetes, Diabetologia 65 (11) (2022) 1867–1882.
[3] L. Zhang, et al., Stem cell therapy in liver regeneration: focus on mesenchymal stem cells and induced pluripotent stem cells, Pharmacol. Ther. 232 (2022) 108004.
[4] X. Li, et al., The role of cancer stem cell-derived exosomes in cancer progression, Stem Cell. Int. 2022 (2022) 9133658.
[5] D.C. Ding, et al., Human umbilical cord mesenchymal stem cells: a new era for stem cell therapy, Cell Transplant. 24 (3) (2015) 339–347.
[6] H. Tang, et al., Mesenchymal stem cell-derived apoptotic bodies: biological functions and therapeutic potential, Cells 11 (23) (2022).
[7] H. Jia, et al., HucMSC exosomes-delivered 14-3-3ζ enhanced autophagy via modulation of ATG16L in preventing cisplatin-induced acute kidney injury, Am J Transl Res 10 (1) (2018) 101–113.
[8] J.H. Wen, et al., Macrophage autophagy in macrophage polarization, chronic inflammation and organ fibrosis, Front. Immunol. 13 (2022) 946832.
[9] E. Barreby, P. Chen, M. Aouadi, Macrophage functional diversity in NAFLD - more than inflammation, Nat. Rev. Endocrinol. 18 (8) (2022) 461–472.
[10] Y. Fu, et al., Umbilical cord mesenchymal stem cells ameliorate inflammation-related tumorigenesis via modulating macrophages, Stem Cell. Int. 2022 (2022) 1617229.
[11] R. Zhao, et al., AQP5 complements LGR5 to determine the fates of gastric cancer stem cells through regulating ULK1 ubiquitination, J. Exp. Clin. Cancer Res. 41 (1) (2022) 322.

[12] B. He, et al., IL-13/IL-13RA2 signaling promotes colorectal cancer stem cell tumorigenesis by inducing ubiquitinated degradation of p53, Genes Dis 11 (1) (2024) 495–508.
[13] B. He, et al., Long noncoding RNA LINC00930 promotes PFKFB3-mediated tumor glycolysis and cell proliferation in nasopharyngeal carcinoma, J. Exp. Clin. Cancer Res. 41 (1) (2022) 77.
[14] F. Barutta, et al., Urinary exosomal microRNAs in incipient diabetic nephropathy, PLoS One 8 (11) (2013) e73798.
[15] S. Thipsawat, Early detection of diabetic nephropathy in patient with type 2 diabetes mellitus: a review of the literature, Diab Vasc Dis Res 18 (6) (2021) 14791641211058856.
[16] L. Dong, S. Pietsch, C. Englert, Towards an understanding of kidney diseases associated with WT1 mutations, Kidney Int. 88 (4) (2015) 684–690.
[17] Y. Wang, et al., Mesenchymal stem cell-derived exosomes ameliorate diabetic kidney disease through the NLRP3 signaling pathway, Stem Cell. 41 (4) (2023) 368–383.
[18] J. Wen, et al., Exosomes in diabetic kidney disease, Kidney Dis. 9 (3) (2023) 131–142.
[19] L.L. Lv, et al., Exosomal miRNA-19b-3p of tubular epithelial cells promotes M1 macrophage activation in kidney injury, Cell Death Differ. 27 (1) (2020) 210–226.
[20] J.L. Liu, et al., Epsin1-mediated exosomal sorting of Dll4 modulates the tubular-macrophage crosstalk in diabetic nephropathy, Mol. Ther. 31 (5) (2023) 1451–1467.
[21] H. Wang, et al., Stem cell-derived exosomal MicroRNAs: potential therapies in diabetic kidney disease, Biomed. Pharmacother. 164 (2023) 114961.
[22] B. He, et al., Hsa_circ_001659 serves as a novel diagnostic and prognostic biomarker for colorectal cancer, Biochem. Biophys. Res. Commun. 551 (2021) 100–106.
[23] R.C. Landis, K.R. Quimby, A.R. Greenidge, M1/M2 macrophages in diabetic nephropathy: nrf2/HO-1 as therapeutic targets, Curr Pharm Des 24 (20) (2018) 2241–2249.
[24] Y. Ma, et al., The influence of angiopoietin-like protein 3 on macrophages polarization and its effect on the podocyte EMT in diabetic nephropathy, Front. Immunol. 14 (2023) 1228399.
[25] Y. Yuan, et al., Mesenchymal stem cells elicit macrophages into M2 phenotype via improving transcription factor EB-mediated autophagy to alleviate diabetic nephropathy, Stem Cell. 38 (5) (2020) 639–652.
[26] C. Moratal, et al., Regulation of monocytes/macrophages by the renin-angiotensin system in diabetic nephropathy: state of the art and results of a pilot study, Int. J. Mol. Sci. 22 (11) (2021).
[27] Y. Shen, et al., A bifunctional fusion protein protected against diabetic nephropathy by suppressing NLRP3 activation, Appl. Microbiol. Biotechnol. 107 (7–8) (2023) 2561–2576.
[28] H. Pan, et al., Serum long non-coding RNA LOC553103 as non-specific diagnostic and prognostic biomarker for common types of human cancer, Clin. Chim. Acta 508 (2020) 69–76.
[29] M. Hara, et al., Urinary podocalyxin is an early marker for podocyte injury in patients with diabetes: establishment of a highly sensitive ELISA to detect urinary podocalyxin, Diabetologia 55 (11) (2012) 2913–2919.
[30] X. Feng, et al., Ferroptosis enhanced diabetic renal tubular injury via HIF-1α/HO-1 pathway in db/db mice, Front. Endocrinol. 12 (2021) 626390.
[31] J. Gagnon, et al., Recommendations of scRNA-seq differential gene expression analysis based on comprehensive benchmarking, Life 12 (6) (2022).
[32] H. Vashistha, et al., Null mutations at the p66 and bradykinin 2 receptor loci induce divergent phenotypes in the diabetic kidney, Am J Physiol Renal Physiol 303 (12) (2012) F1629–F1640.
[33] Y. Zhang, et al., Exosomes derived from human umbilical cord blood mesenchymal stem cells stimulate regenerative wound healing via transforming growth factor-β receptor inhibition, Stem Cell Res. Ther. 12 (1) (2021) 434.
[34] Y. Xu, et al., HucMSC-Ex carrying miR-203a-3p.2 ameliorates colitis through the suppression of caspase11/4-induced macrophage pyroptosis, Int Immunopharmacol 110 (2022) 108925.
[35] B. He, et al., Epstein-Barr virus-encoded miR-BART6-3p inhibits cancer cell metastasis and invasion by targeting long non-coding RNA LOC553103, Cell Death Dis. 7 (9) (2016) e2353.
[36] Y. Hao, et al., Nuclear translocation of p85β promotes tumorigenesis of PIK3CA helical domain mutant cancer, Nat. Commun. 13 (1) (2022) 1974.
[37] B. He, et al., Arachidonic acid released by PIK3CA mutant tumor cells triggers malignant transformation of colonic epithelium by inducing chromatin remodeling, Cell Rep Med 5 (5) (2024) 101510.